Proceedings of the ASME 2023
50th Annual Review of Progress in
Quantitative Nondestructive Evaluation
QNDE2023
July 24-27, 2023, Austin, Texas

QNDE2023-108287

ENTIRE TORQUE RANGE MONITORING OF BOLTED JOINTS VIA NONLINEAR ELECTROMECHANICAL IMPEDANCE SPECTROSCOPY (NEMIS)

Runye Lu
University of Michigan-Shanghai Jiao Tong University Joint Institute, Shanghai Jiao Tong University, Shanghai, China

Yanfeng Shen
University of Michigan-Shanghai Jiao Tong University Joint Institute, Shanghai Jiao Tong University, Shanghai, China

ABSTRACT

This paper proposes a Nonlinear Electro-mechanical Impedance Spectroscopy (NEMIS) methodology for the entire torque range monitoring of bolted joints. NEMIS utilizes a temporal interrogative signal to obtain the nonlinear impedance spectrum. It is capable of evaluating the structural resonance information as the conventional EMIS does and capturing the Contact Acoustic Nonlinearity (CAN) features simultaneously with only a single Piezoelectric Wafer Active Sensor (PWAS). A comparative illustration of the underlying mechanism behind the conventional EMIS, nonlinear ultrasonic techniques, and the proposed NEMIS was conducted. Subsequently, a reduced-order analytical model was established to simulate the variable rough interfaces of the bolted joints at different looseness stages. Parametric studies were carried out on the model to demonstrate the higher harmonics and vibro-acoustic modulation features from the bolt looseness. Ultimately, the experimental implementation of NEMIS for the entire torque range monitoring of a bolted joint was performed and compared with the conventional EMIS method. It was proved that NEMIS could detect both the incipient bolt loosening at an embryo stage and severe loosening of the bolted joints at the terminal period, combining the merits of the conventional EMIS and the nonlinear ultrasonic methodology. The paper finishes with summary, concluding remarks, and suggestions for future work.

Keywords: bolt loosening; electro-mechanical impedance spectroscopy; nonlinear ultrasonics; higher harmonics; contact acoustic nonlinearity; structural health monitoring

1. INTRODUCTION

Bolted joints have been ubiquitously employed for the detachable assembly of interconnecting structures [1]. The past decades have witnessed a skyrocketing application of bolted joints on versatile engineering structures [2]. The extensive deployment is usually accompanied by the tremendous potential failure. Throughout the service span of a bolted structure, external loadings, inappropriate manipulations, and environmental invasions may inevitably cause the loosening of bolted joints, triggering catastrophic failures, thus causing loss of properties and even lives [3]. Taking the safety issue as the dominating priority, early awareness of bolt loosening and continuous monitoring of bolt tightness are of superior significance [4].

Unremitting endeavors have been devoted to the development of the structural health monitoring (SHM) techniques for bolt loosening evaluation. Several SHM methodologies have been demonstrated to be effective for the detection of bolt loosening like vibration-based method, electromechanical impedance-based techniques, and guided wave-based approaches including linear and nonlinear ultrasonics [2]. Regarding the vibration-based technique, features like resonant frequencies and mode shapes are utilized for the detection of bolt loosening [5]. However, these global dynamic features are not sensitive enough for the perception of local structural dynamic changes arising from local and early stage bolt loosening [6]. Electromechanical impedance (EMI) method couples the mechanical impedance with electrical impedance at the piezoelectric active wafer sensor (PWAS) terminal [7-9]. A full-scale test was performed by Pavelko on the aircraft bolted joints via EMI method [10, 11]. Despite the feasibility of the EMI method detecting the existence of bolt loosening, the required impedance analyzer is usually bulky and expensive, which means it is not portable and cost-effective [12]. Linear guided wave-based ultrasonics, utilizing features like time-of-flight (ToF) variations [13, 14], mode conversion [15, 16], and wave attenuation [17], arouse researchers' interest. Wang et al. demonstrated the feasibility of time reversal method to monitor the bolted joints [18]. A new acoustic emission strategy was also applied to multi-bolt looseness monitoring [19].Guided wave energy transmitted through the bolted joints is

relevant to the contact status of bolt interfaces, known as wave energy dissipation (WED) method. Yang and Chang investigated the preload level and location of the loosening bolts via transmitted energy and attenuation [5, 20]. It was found that the WED would not change when the applied torch reached a saturation status [21]. The signal features are not sufficiently distinctive to indicate an embryo stage of bolt looseness, imposing a bottleneck on the linear ultrasonic methodologies [22].

To circumvent the deficiencies of linear guided wave approaches, researchers have concentrated on the nonlinear ultrasonic methods [23, 24]. Nonlinear signal features like subharmonic resonance [25], second harmonic generation (SHG) [26] and higher-order harmonics [27, 28], and vibro-acoustic modulation (VAM) [27, 29-31] are exploited for the implementation of early awareness of the bolt loosening. To further understand the mechanism behind the nonlinear response of bolted joints, theoretical models were established to simulate the bolt interface behaviors. Zhang et al. adopted a reduced-order two-DOF nonlinear model to demonstrate the physical phenomena [25]. In reality, the surfaces of the two adjacent components are rough, with an irregular contact condition. An analytical 1-D vibration model was proposed based on the micro-contact theory regarding the rough contact surfaces by Zhang et al. [27]. Furthermore, a 3-D finite element (FE) model was proposed to simulate the microscopic roughness of bolted joints by applying the fractal contact theory, regarding the rough surfaces as a problem of stochastic process [32]. Yang et al. utilized SHG and demonstrated that the magnitude of the SHG increased with the loosening of the bolted joint [26]. Despite the superb sensitivity and promising feasibility of SHG, it possessed great uncertainty and unreliability. Electronic instrument may bring about inherent higher harmonics which is unavoidable and can result in false alarm [33]. In comparison, the essence of the VAM method resides on the CAN induced by the interaction of interfacial contact behaviors with a mixed excitation, which consists of a pumping vibration signal and a probing wave signal [29, 34]. The VAM method captured steady-state vibration responses generated by the harmonic pumping excitation, which is immune to measurement noise and environmental influence [29]. However, one common disadvantage of the spectral sideband techniques lies in that two or more sensors are indispensable to form the pitch-catch mode or sensors array for the effective implementation [28]. Moreover, for the majority of current nonlinear ultrasonic methods, they are incapable of detecting sudden serious bolted joints damages of a macro scale, which cannot trigger nonlinear features arising from an appropriate contact situation. It should be noted that a hybrid use of WED and VAM was proposed and compared by Zhang et al. [31], yet it still rely on multiple sensors to cooperate.

It can be concluded that linear methods are incapable of monitoring the embryo stage of bolt loosening. However, they are effective when the bolted joints become further loosened or when the bolted structures suddenly suffer serious damage. Regarding the nonlinear methodologies, despite their prowess in detecting the incipient bolt looseness, they could be blind after a certain level of loosening. If a bolted structure encounters a sudden impact and the bolted joints become totally loosened or damaged, the nonlinear ultrasonic techniques would not be able to evaluate the change. In order to conduct the entire torque range monitoring of the bolted joints, this paper proposes a nonlinear electromechanical impedance spectroscopy (NEMIS) methodology, exploiting the strengths of the linear and nonlinear methods and compensate for each other's the limitations. It can obtain the equivalent EMI spectrum (linear analysis) and capture the nonlinear ultrasonic features (nonlinear analysis) simultaneously. The EMI spectrum evaluates the bolt loosening level by the deviation of the structural resonance peaks. The nonlinear ultrasonic features detect the existence of CAN arising from the incipient loosening of the bolted joints. This endows NEMIS with the distinctive ability to monitor the bolt loosening from an initially tight stage until the bolted joints become totally loosened or even damaged, covering the whole service span.

This paper starts with the illustration of the mechanism behind the proposed NEMIS by the comparison with the conventional EMIS method and nonlinear ultrasonic method. Afterwards, an analytical reduced-order model was established to simulate the rough contact interfaces of the bolted joints. Numerical studies were conducted to demonstrate the changes of linear and nonlinear features resulting from the loosening of bolted joints. Afterwards, systematic experiments were performed to showcase the performance of NEMIS for the entire service span monitoring for the bolt looseness.

2. COMPARATIVE ILLUSTRATION OF MECHANIS M BEHIND NEMIS

This section illustrates the mechanism behind the proposed NEMIS method, in comparison with the conventional EMIS method and nonlinear ultrasonic techniques. The conventional EMIS conducts the analysis in the frequency domain utilizing a stepwise sweeping excitation with a single PWAS transducer. It excites the bolted structure with a sinusoid voltage signal at a certain frequency and subsequently captures the steady-state electrode response at the PWAS terminal, from which a single electromechanical impedance value can be measured. By repeating the procedure from a low frequency to a high frequency, the impedance spectrum of a certain frequency range can be obtained by composing each steady-state response, as displayed in Figure 1(a). The structural resonance information can be extracted from the impedance spectrum to monitor the bolt looseness. Regarding the nonlinear ultrasonic methodology, usually two PWAS transducers are required to form a pitch-catch mode, where one PWAS functions as the actuator and another plays the role of the receiver. Taking the typical excitation signal as an example, as observed in Figure 1(b), a low-frequency pumping signal and a high-frequency probing signal are combined to excite the transmitter. After the wave interacting with the bolted interfaces, the temporal response containing time-history wave-structural interaction information would be capture by the receiver PWAS. Ultimately, nonlinear ultrasonic features like second harmonic generation (SHG) and vibro-acoustic modulation (VAM) can be obtained.

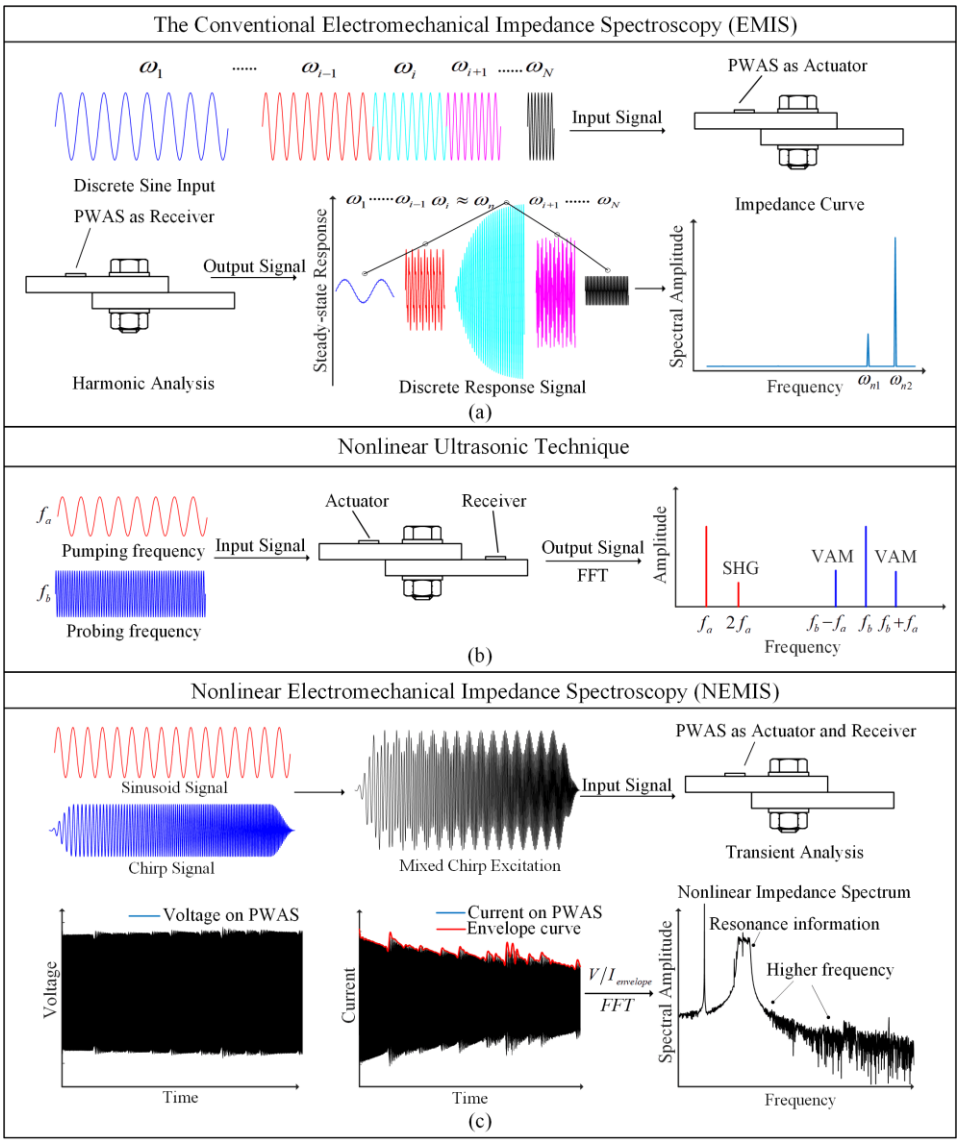

FIGURE 1: THE MECHANISM AND PROCEDURES BEHIND (A) THE CONVENTIONAL EMIS; (B) NONLINEAR ULTRASONIC TECHNIQUE; (C) NEMIS

To embrace the merits of the EMIS and nonlinear ultrasonic methodology and circumvent the limitations, the nonlinear electromechanical impedance spectroscopy (NEMIS) is proposed to conduct the bolt looseness monitoring covering the whole torque range. Different from the aforementioned two methods, NEMIS employs a temporal sweeping chirp signal combined with a sinusoid signal, which contains rich time-history information and meanwhile covers a large frequency band. Therefore, NEMIS is capable of obtaining the structural resonance information and capturing the nonlinear ultrasonic features. That is to say, the change of local stiffness resulting from the bolted joints looseness can be mirrored through the shift of the impedance spectrum, while the nonlinear signatures are exploited to detect the early-stage loosening of the bolt. The two features could cooperate with each other to establish an all-round and comprehensive monitoring strategy, as shown in Figure 1(c).

3. ANALYTICAL CAN MODEL AND CORRESPOND ING PARAMETRIC STUDIES

A reduced-order theoretical CAN model was established, simulating the rough interface dynamics under different loosening conditions by exploiting a transitional stiffness region. Afterwards, the central difference (CD) computation method was applied to conduct the parametric studies.

CAN originates from the contact behaviors when two interfaces experience periodic collisions and oscillations, where the local structural stiffness is altered according to the contact conditions, as depicted in Figure 2(a). When the oscillation interacts with bolted joints, the compressional part tends to close the interfaces as a continuum, giving rise to a higher stiffness. In

comparison, the tensile component inclines to separate the bolted interfaces, rendering a relatively low stiffness. A nonlinear oscillator model was established to capture the rough contact surfaces and different levels of bolt loosening conditions utilizing a transition stiffness region, as illustrated in Figure 2(b)

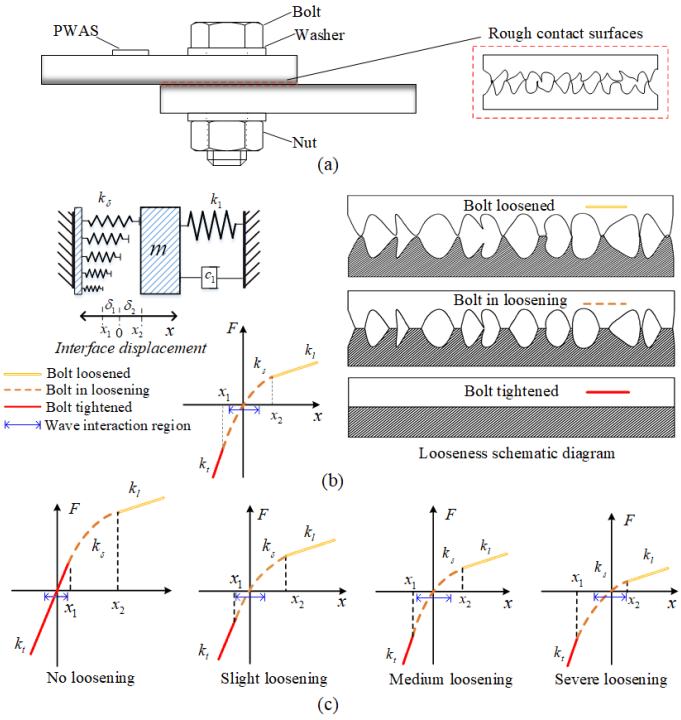

FIGURE 2: (A) THE SCHEMATIC DIAGRAM OF BOLTED JOINTS; (B) THE REDUCED-ORDER CAN OSCILLATOR MODEL SIMULATING THE BOLT LOOSENING; (C) THE FORCE-DISPLACEMENT RELATIONSHIP AT DIFFERENT LOOSENING LEVELS.

The transitional stiffness region covers the loosening situation after the initiation of bolt loosening and before the bolted joints are totally loosened. The length of the region simulating the rough contact surfaces is quantified by the parameter δ, which is determined by the critical coordinates, x_1 and x_2. The force-displacement curve in Figure 2(b) illustrates that when the bolted joints interfaces oscillate and interact with each other, the rough contact surfaces will result in a continuously changing stiffness k_δ. The critical stiffness is determined by k_t and k_l respectively. k_t represents the structural stiffness when the bolted joint is fully tightened while k_l signifies the stiffness when the bolt is totally loosened. The overall structural stiffness follows a polynomial expression:

$$k(x_i)=\begin{cases} k_t = max(k_\delta), & x_i \le x_1 \\ k_t - \dfrac{x_1(k_l-k_t)}{x_2-x_1} + \dfrac{2(k_l-k_t)}{x_2-x_1}x_i, & x_1 \le x_i \le x_2 \\ k_l = min(k_\delta), & x_2 \le x_i \end{cases} \quad (1)$$

where x_i represents the displacement response at the *i-th* time step in the CD computation procedure.

The level of the bolt looseness is defined by the drifting of the force-displacement curves as illustrated in Figure 2(c). Under a certain amplitude of the preload, the interaction region (marked by the blue line with arrows) dwells in different sections of the force-displacement curve, corresponding to the different levels of bolt loosening. When the bolted joints are tightened, the stiffness keeps a constant value, rendering a linear displacement response. Once loosened, the interaction region would overlap with the transitional region, generating a response containing nonlinear features. With the severity of bolt looseness increasing, the force-displacement curve displays a leftward and downward deviation, and therefore the average stiffness during the wave interaction region becomes smaller.

Regarding the case study on the bolt loosening, the structural information is determined by the following parameters. The natural frequency f_t, equals to 200 kHz when the bolted joint is tightened as a continuum while the natural frequency, f_l, drops to 160 kHz when the bolt is totally loosened. The aforementioned k_t and k_l correspond to the stiffness at the two critical situations. For the excitation, it was composed of a chirp signal sweeping from 140 kHz to 220 kHz and a pumping sinusoid signal of 30 kHz, covering the two critical frequencies to better manifest the resonance information changes. The sinusoid pumping signal was employed to modulate with the chirp signal to generate the VAM features. The frequency spectra of the displacement response for different loosening stages were derived and displayed in Figure 3. For the tightened condition, the frequency components were consistent with the external excitation, from 140 kHz to 220 kHz. The resonance peak was located at 200 kHz, identical to the natural frequency of the tightened bolted joints. Upon the occurrence of the bolt loosening, nonlinear features began to emerge, including second harmonic generation (SHG: 60 kHz and 280-440 kHz) and vibro-acoustic modulation (VAM). The VAM between the pumping frequency and chirp frequency was much more complicated, since it also comprised the modulation between fundamental frequency components and higher order frequency components, as marked in Figure 3. With the increment of the bolt loosening level, the relative amplitude of SHG and VAM displayed an increasing trend. Meanwhile, the change of linear features was mirrored into the leftward shift of the resonance peak, indicating the loss of overall structural stiffness.

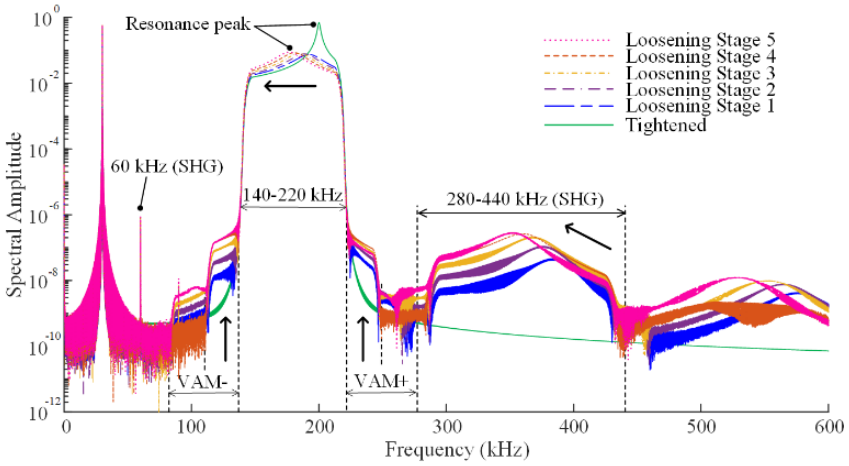

FIGURE 3: THE NONLINEAR FREQUENCY SPECTRA FOR DIFFERENT BOLT LOOSENESS LEVELS

4. COMPARATIVE EXPERIMENTAL INVESTIGATI ON FOR MONITORING OF BOLT LOOSENING

This section presents a comparative experimental investigation on the performance of bolt loosening monitoring to demonstrate the superiority of the proposed NEMIS method. Firstly, the conventional EMIS, representing the linear regime, was conducted. The linear analysis was capable of monitoring the serious blot looseness level at the terminal period instead of the embryo stage of bolt loosening. Then, the proposed NEMIS was carried out for the comprehensive monitoring of the bolt looseness covering the complete torque span of the bolted joints. Results from the two methods were analyzed and compared.

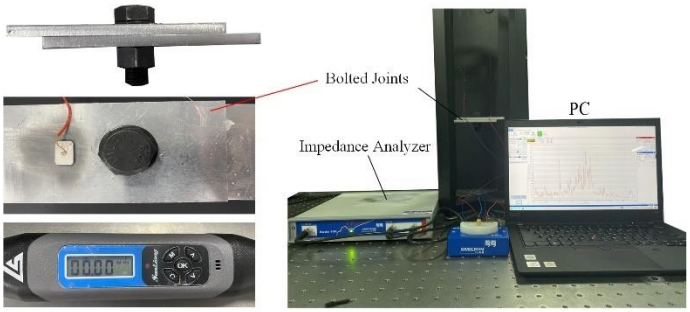

FIGURE 4: (A) THE BOLTED JOINTS AND THE TORQUE WRENCH; (B) THE EXPERIMENTAL SETTING FOR THE CONVENTIONAL EMIS METHOD

The experimental layouts for the EMIS method and the NEMIS method were displayed in Figure 4 and Figure 5, respectively. For the experimental setting of the conventional EMIS, the impedance analyzer (Omicron Bode 100) was utilized to measure the structural electromechanical impedance spectrum for the linear analysis. The applied bolt was M12 and made of steel (C45e4), connecting two aluminum beams ($120\times50\times5$ mm^3, Al 6061) with a single-lap connection, as can be shown in Figure 4(a). The size of the PWAS transducer was $14.4\times9.7\times1.5$ mm^3 and it was made of APC-850. The torque was exerted by the torque wrench with electronic readings (Sanliang SLH-60). The Al-Al joint was suspended on the fixing shelf to simulate a free-free boundary condition, as displayed in . The computer was connected to the impedance analyzer to capture and record the impedance spectral readings.

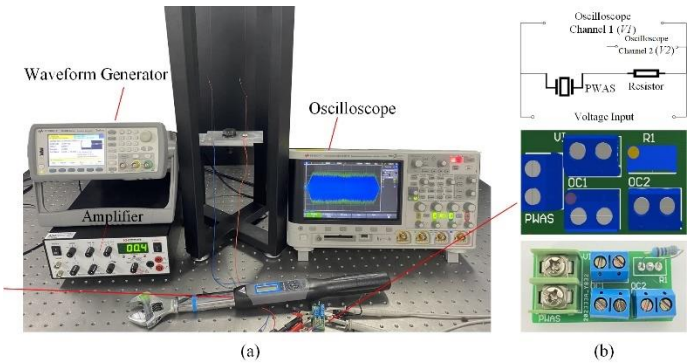

FIGURE 5: (A) THE OVERALL EXPERIMENTAL SETTING FOR THE NEMIS METHOD; (B) THE BOLTED JOINTS AND THE TORQUE WRENCH; (C) THE TAILORED AUXILIARY CIRCUIT

Regarding the experimental setting for NEMIS, as shown in Figure 5(a), the waveform generator (KEYSIGHT 33500B Series) was employed to input the excitation signal through the power amplifier (KROHN-HITE LQ1801R) to the bolted joint. The length of the specimen is relatively short to demonstrate the capability of functioning with the interference from the boundary reflection. The oscilloscope (KEYSIGHT DSO-X 3014T) was applied to measure the response voltage signal. Particularly, a tailored auxiliary circuit was designed to capture the voltage and current at the PWAS terminal, which was displayed in Figure 5 (b).

4.1. Analysis of Conventional EMIS Method

Different levels of the torque were exerted on the bolted joints by the torque wrench from 0 Nm to 60 Nm at a step of 5 Nm to represent different bolt looseness states, including a totally loosened state. At each torque value, the structural impedance spectrum from 380 kHz to 420 kHz was measured by the impedance analyzer, as can been observed in Figure 6.

The major resonance peaks located around 400 kHz, with several concomitant resonance peaks existing nearby. The resonance peaks denoted the natural frequency of the bolted structure, which was determined by the local nominal material and geometric parameters. When the bolted joints were tightened gradually, the local stiffness was enhanced, thus resulting a rightward deviation of the resonance peak. Besides, the amplitude of the response signal was lowered due to the increment of the stiffness, which was also reflected in the impedance spectra. However, there existed a saturation state, where the structural resonance peaks would no longer shift with the increasing torque. The bolted joint with the torque of 60 Nm was thought as the totally tightened case, i.e., the pristine case. The impedance spectra at other torque levels were compared with the spectrum of the pristine case to evaluate severity of the bolt loosening. The quantitative evaluation was conducted using the RMSD value given in Eq (2).

$$\mathrm{RMSD} = \sqrt{\sum_{f=380kHz}^{f=420kHz} (\mathrm{Im}_i - \mathrm{Im}_i^0)^2 \Big/ \sum_{f=380kHz}^{f=420kHz} (\mathrm{Im}_i^0)^2} \tag{2}$$

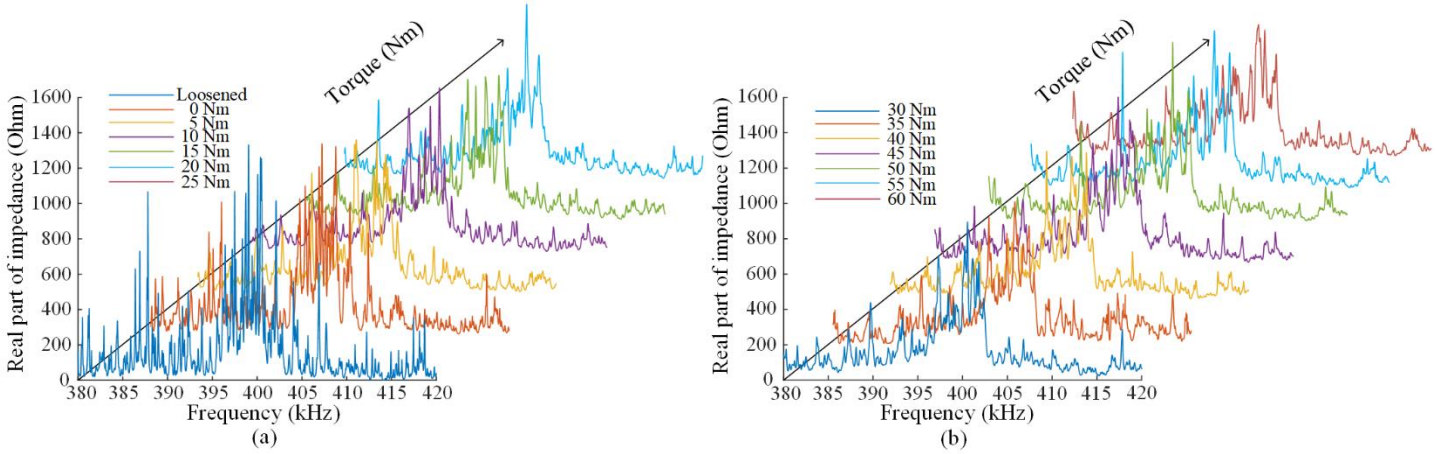

FIGURE 6: THE ELECTROMECHANICAL IMPEDANCE SPECTRA FOR THE TORQUE FROM 0 NM TO 60 NM

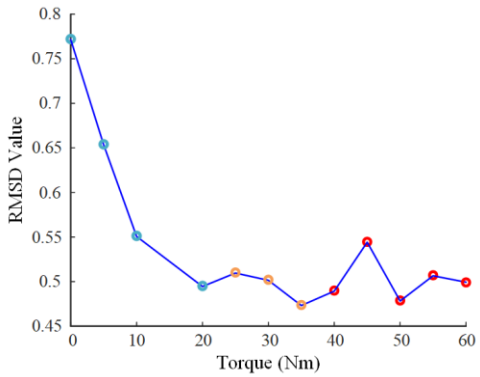

FIGURE 7: THE RMSD CURVE FOR IMPEDANCE SPECTRA UNDER DIFFERENT TORQUE LEVELS

As can be observed in Figure 7, the RMSD value generally decreased with the torque increment below 35 Nm and was monotonously decreasing below 20 Nm. When the bolted joint became tightened after applying a torque over 35 Nm, the curve displayed an irregular trend, indicating a saturation state had been reached. It can be concluded that under the torque of 20 Nm, the conventional EMIS could effectively monitor the looseness condition of the bolt, while it could not work well beyond 35 Nm. Unfortunately, the embryo period of the bolt loosening usually happens at a slightly lower value than the totally tightened state (60 Nm). Therefore, the linear EMIS method only possesses the capability of monitoring the serious bolt looseness at the latter stage and is not sensitive for the incipient bolt loosening.

4.2. Verification and Application of NEMIS for Monito ring of Bolt Loosening

This section aims at illustrating the procedures to derive the nonlinear impedance spectra for NEMIS, which has been displayed in Figure 1(c). To start, the excitation signal was the superposition of a 50 kHz sinusoid pumping signal and a chirp sweeping from 380 kHz to 420 kHz, identical to the frequency band of the conventional EMIS method. By utilizing the auxiliary series circuit, the overall voltage response and the voltage on the resistor could be obtained as showcased in Figure 8(a). Subtracting voltage 2 from voltage 1 ($V_{PWAS} = V_2 - V_1$), the temporal voltage response at the PWAS terminal could be derived. Simultaneously, the envelope curve of V_{PWAS} could be obtained by the Hilbert transform. Afterwards, the electrical

current at the series circuit could be measured by dividing the voltage 2 over the resistor value ($I = V_2 / R_{resistor}$). Then, dividing the voltage envelope signal by the temporal current response ($Z = V_{amplitude} / I$), the temporal impedance response could be obtained. Applying Fast Fourier Transform (FFT) on the temporal impedance response, the final nonlinear impedance spectrum could be derived as Figure 8(d) after processing.

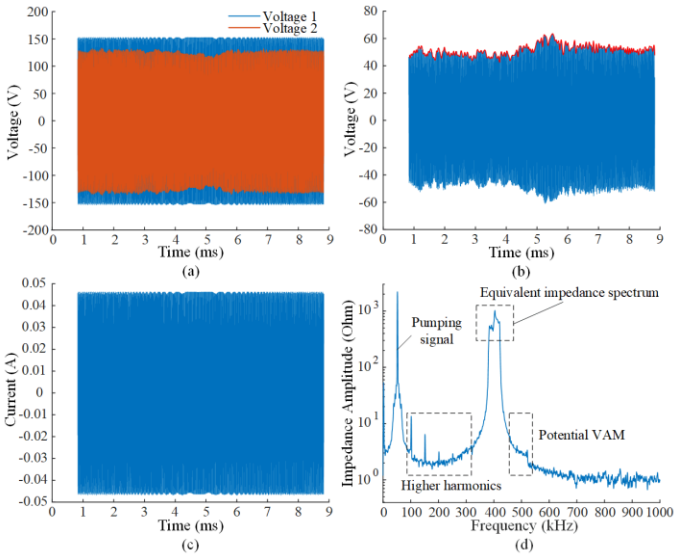

FIGURE 8: THE VARIABLES FOR THE DERIVATION OF NONLINEAR IMPEDANCE SPECTRUM (A) TEMPORAL VOLTAGE RESPONSE IN CHANNEL 1 AND CHANNEL 2; (B) TEMPORAL VOLTAGE RESPONSE AT THE PWAS TERMINAL; (C) TEMPORAL CURRENT RESPONSE AT THE PWAS TERMINAL; (D) THE NONLINEAR IMPEDANCE SPECTRUM

This nonlinear impedance spectrum was the essence of NEMIS due to its capability of conducting linear and nonlinear analysis simultaneously. For the linear part, the spectrum of the chirp excitation frequency (from 380 kHz to 420 kHz) could play the equivalent role as the conventional impedance spectrum shown in Figure 6, which would deviate due to the change in the structural resonance information. The accuracy and the feasibility of the equivalent chirp impedance spectrum were verified in Figure 9. The green solid impedance spectrum of the conventional EMIS method was obtained from the impedance analyzer, which was considered as the standard version. The brown dotted curve represented the original equivalent impedance spectrum from the NEMIS method. To better evaluate the resonance deviation and avoid the signal noise disturbance, the original spectrum was further processed with a smoothing filter. The processed blue dashed curve denoted the spectrum after smooth processing, which was identical to that in Figure 8(d) within the swept frequency range. The amplitude difference was due to the fact that NEMIS captured the instantaneous response, while EMIS captured the steady-state response. Despite the amplitude difference, the key features such as the location of the resonance peaks for both spectra were in good agreement with each other, demonstrating the feasibility of the equivalent impedance spectrum. Furthermore, for the nonlinear part, the pumping sinusoid signal could generate higher harmonics and vibro-acoustic modulation (VAM) with the chirp signal, as marked in Figure 8(d). These distinctive nonlinear features could be utilized for the monitoring of the early-stage bolt looseness.

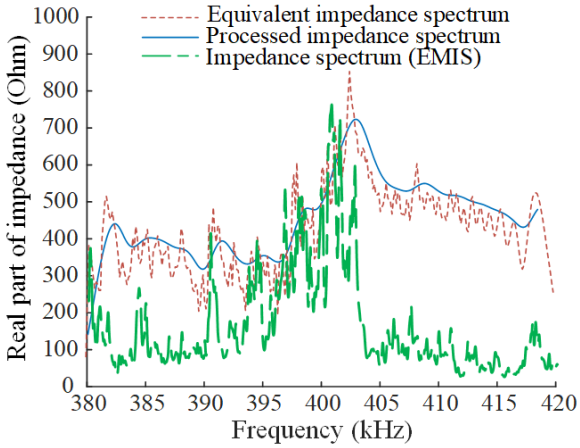

FIGURE 9: VERIFICATION OF THE EQUIVALENT IMPEDANCE SPECTRUM AGAINST THE CONVENTIONAL IMPEDANCE SPECTRUM FROM THE IMPEDANCE ANALYZER

The nonlinear impedance spectrum was then exploited to conduct both linear analysis and nonlinear analysis simultaneously for monitoring the entire torque range of the bolt joint. Following the aforementioned procedure, an increasing torque from 0 Nm to 60 Nm was exerted on the bolted joint at an interval of 5 Nm, including a totally loosened case. At each torque level, the nonlinear impedance spectrum was derived. The experiment was repeated for ten times to avoid the stochastic perturbation. The equivalent chirp impedance spectrum from 380 kHz to 420 kHz was utilized to monitor the medium and severe bolt looseness due to its sensitivity to the local stiffness change, which would cause the deviation of the structural resonance peaks. Meanwhile, the higher harmonic generation was employed to monitor the early-stage loosening. The logic and strategy behind the NEMIS method for monitoring the entire service torque range of the bolt is stated as below. The nonlinear ultrasonic features were utilized first to monitor the existence of the early-stage loosening. Once receiving the initial alarm for slight loosening, the equivalent impedance spectra were then exploited for the subsequent and consecutive evaluation. The nonlinear spectra of the bolted joint under different loosening conditions from one typical experiment were selected and displayed in Figure 10. It is worth mentioning that the spectra were separated with the vertical shift to make it clear to be observed.

Following the previous strategy, the nonlinear ultrasonic features should be scrutinized first. It is noteworthy that there existed second harmonic component (100 kHz) and vibro-acoustic modulation frequency components (280 kHz- 320 kHz

and 480 kHz- 520 kHz) for all the spectra, which were resulted from the inherent nonlinearity from the instrument. To avoid being influenced by the inherent nonlinear sources, the third harmonic (150 kHz) and fourth harmonic (200 kHz) components were examined. It can be observed that for the fully tightened bolted joints (at torque over 45 Nm), almost no nonlinear feature was generated. As the applied torque decreased below 40 Nm, the third harmonics and the fourth harmonics began to emerge, then peaked at the torque 35 Nm, and culminated with the torque of 20 Nm, after which, the higher harmonic components disappeared. The mechanism behind the phenomena can be explained by the contact acoustic nonlinearity (CAN) originated from the rough joints interfaces as mentioned in the theoretical model. The intensity of CAN skyrocketed at the embryo of the bolt loosening and diminishes when the looseness aggravated to a severe level. The increasing gap between the interfaces inhibited the generation of the contact behaviors.

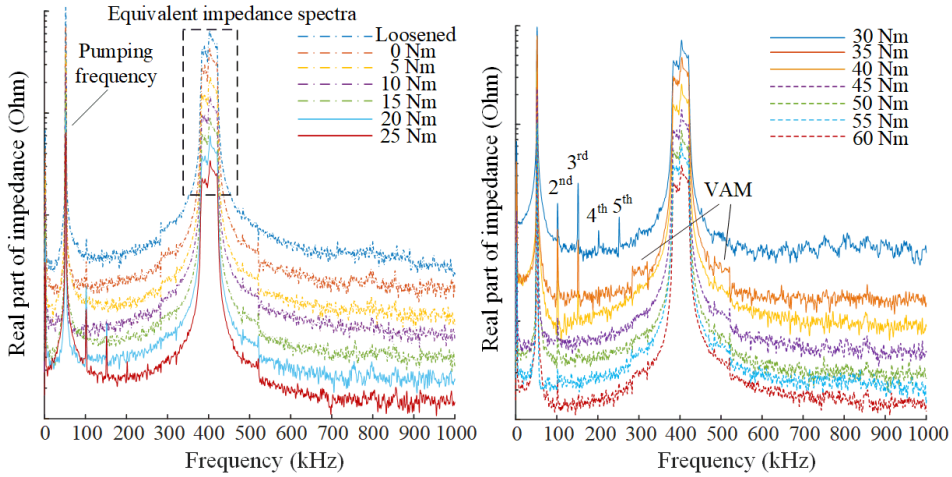

FIGURE 10: THE NONLINEAR IMPEDANCE SPECTRA FOR BOLTED JOINTS WITH DIFFERENT APPLIED TORQUES (WITH VERTICAL AMPLITUDE SHIFT)

Regarding the equivalent impedance spectra (380 kHz to 420 kHz) for linear analysis, the subtle differences could not be observed directly from Figure 10, so the zoom-in vision was displayed in Figure 11. The case under the torque of 60 Nm was taken as the pristine case to be compared with. The observation revealed that with the increment of applied torque, the local structural stiffness was elevated, thus rendering the overall rightward and downward deviation of the impedance spectra.

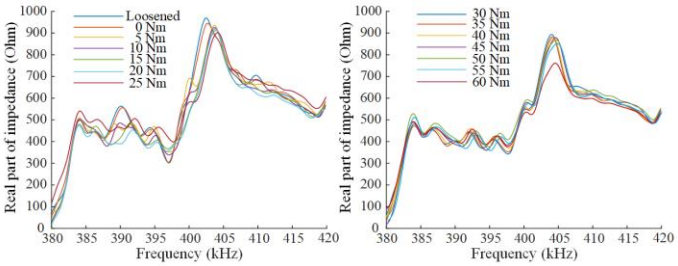

FIGURE 11: THE EQUIVALENT IMPEDANCE SPECTRA FOR THE BOLTED JOINTS UNDER DIFFERENT TORQUE VALUES (EXTRACTED FROM THE NONLINEAR IMPEDANCE SPECTRA BETWEEN 380 KHZ-420 KHZ)

To quantitatively evaluate the intensity of the nonlinearity, the relative amplitude of the third and fourth harmonics against the amplitude of the pumping frequency were evaluated and regarded as the loosening index as shown in Figure 12. The boxplot was utilized to statistically mirror the tendency of nonlinearity for the ten repetitive experiments. On each box, the central mark indicated the median, and the bottom and top edges of the box denoted the 25th and 75th percentiles, respectively. The whiskers extended to the most extreme data points without considering the outliers, and the outliers were plotted individually using the '+' symbol. The observation revealed that the index value drastically increased below the threshold torque of 40 Nm, indicating that the embryo stage of the bolt loosening happened at the torque from 30 Nm to 40 Nm in the ten experiments. The loosening index remained a relatively low value below 25 Nm without a monotonous change when the bolted joints were considered loosened to a medium and severe level. Under such circumstance, the nonlinear part of NEMIS was not sensitive anymore.

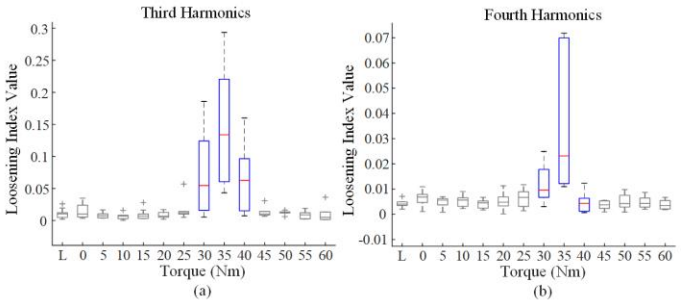

FIGURE 12: THE LOOSENING INDEX BOXPLOT OF THE THIRD HARMONICS AND THE FOURTH HARMONICS

Therefore, the equivalent impedance spectra (linear part) were then utilized to conduct the subsequent monitoring of the bolt looseness. The increasing severity of the bolt looseness rendered a leftward and upward of the impedance spectral variation. Such deviation was quantified by the root mean square deviation (RMSD), the boxplot of which was illustrated in Figure 13. Generally, the mean value of RMSD displayed a monotonously increasing trend as the applied torque decreased. Once the nonlinear analysis raised the alarm for slight bolt loosening, for example, under the torque of 35 NM, the RMSD could evaluate the moderate and severe loosening afterwards. To sum, the nonlinear analysis and linear analysis utilizing the nonlinear impedance spectra are endowed with mutual complementary characteristics and can therefore conduct the comprehensive monitoring of the bolt loosening, from the early stage to severe stage.

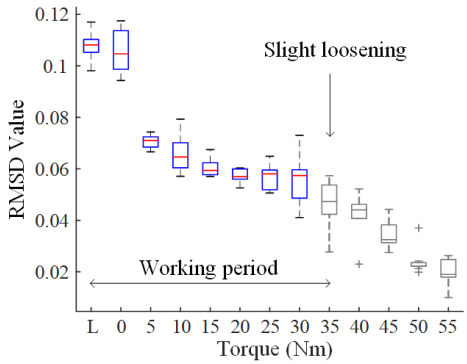

FIGURE 13: RMSD BOXPLOT FOR THE EQUIVALENT IMPEDANCE SPECTRA OF THE LINEAR ANALYSIS

5. CONCLUDING REMARKS

This paper proposed a NEMIS methodology for the entire torque range monitoring of the bolt. The comparative illustration proved the superiority of the NEMIS over the other methods. The analytical model and the corresponding numerical case studies demonstrated the linear and nonlinear features from bolt loosening. The experiment proved that NEMIS could effectively detect the embryo stage loosening of the bolted joints and function as an alarm to initiate the subsequent monitoring to continuously monitor the bolt loosening at the terminal period until total looseness. Therefore, NEMIS succeeded in covering entire service torque span of the bolted joints, establishing an all-around and comprehensive strategy for monitoring the bolt looseness.

6. ACKNOWLEDGEMENTS

The support from the National Natural Science Foundation of China (contract numbers 51975357 and 51605284) is thankfully acknowledged; this research is also sponsored by the Shanghai Rising-star Program (contract number 21QA1405100).

REFERENCES

[1] Ibrahim, R., and Pettit, C., 2005, "Uncertainties and dynamic problems of bolted joints and other fasteners," Journal of Sound and Vibration, 279, pp. 857-936.
[2] Du, F., Xu, C., Ren, H., and Yan, C., 2018, "Structural Health Monitoring of Bolted Joints Using Guided Waves: A Review," Structural Health Monitoring from Sensing to Processing.
[3] Wang, T., Song, G., Liu, S., Li, Y., and Xiao, H., 2013, "Review of Bolted Connection Monitoring," International Journal of Distributed Sensor Networks, 9(12).
[4] He, Y., Xiao, Y., Su, Z., Pan, Y., and Zhang, Z., 2022, "Contact acoustic nonlinearity effect on the vibro-acoustic modulation of delaminated composite structures," Mechanical Systems and Signal Processing, 163.
[5] Yang, J., and Chang, F.-K., 2006, "Detection of bolt loosening in C–C composite thermal protection panels: I. Diagnostic principle," Smart Materials and Structures, 15(2), pp. 581-590.
[6] Todd, M., Nichols, J., Nichols, C., and Virgin, L., 2004, "An assessment of modal property effectiveness in detecting bolted joint degradation: Theory and experiment," Journal of Sound Vibration, 275, pp. 1113-1126.
[7] Lu, R., Shen, Y., Qu, W., and Xiao, L., 2022, "Health monitoring of high-damping viscoelastic materials using sub-resonator enriched electro-mechanical impedance signatures," Smart Materials and Structures, 31(9), p. 095046.
[8] Venu Gopal Madhav, A., and Chee Kiong, S., 2009, "Application of Electromechanical Impedance Technique for Engineering Structures: Review and Future Issues," Journal of Intelligent Material Systems and Structures, 21(1), pp. 41-59.
[9] Gresil, M., Yu, L., Giurgiutiu, V., and Sutton, M., 2012, "Predictive modeling of electromechanical impedance spectroscopy for composite materials," Structural Health Monitoring: An International Journal, 11(6), pp. 671-683.
[10] Pavelko, I., Pavelko, V., Kuznetsov, S., and Ozolinsh, I., 2014, "Bolt-joint structural health monitoring by the method of electromechanical impedance," Aircraft Engineering and Aerospace Technology, 86, pp. 207-214.
[11] Yu, T. Y., Pavelko, V., Gyekenyesi, A. L., Shull, P. J., Diaz, A. A., Wu, H. F., and Aktan, A. E., 2013, "Electromechanical impedance for SHM of aircraft bolted joints," Nondestructive Characterization for Composite Materials, Aerospace Engineering, Civil Infrastructure, and Homeland Security 2013.
[12] Park, G., Sohn, H., Farrar, C. R., and Inman, D. J., 2003, "Overview of Piezoelectric Impedance-Based Health Monitoring and Path Forward," The Shock and Vibration Digest, 35, pp. 451-463.
[13] Jhang, K.-Y., Quan, H.-H., Ha, J., and Kim, N.-Y., 2007, "Estimation of clamping force in high-tension bolts through ultrasonic velocity measurement," Ultrasonics, 44 Suppl 1, pp. e1339-1342.
[14] Miller, T. H., Kundu, T., Huang, J., and Grill, J. Y., 2012, "A new guided wave–based technique for corrosion monitoring in reinforced concrete," Structural Health Monitoring, 12(1), pp. 35-47.

[15] Yang, Z., Radzienski, M., Kudela, P., and Ostachowicz, W., 2016, "Fourier spectral-based modal curvature analysis and its application to damage detection in beams," Mechanical Systems and Signal Processing, 84.
[16] Wang, K., Liu, M., Cao, W., Yang, W., Su, Z., and Cui, F., 2019, "Detection and sizing of disbond in multilayer bonded structure using modally selective guided wave," Structural Health Monitoring, 20(3), pp. 904-916.
[17] Mei, H., and Giurgiutiu, V., 2018, "Guided wave excitation and propagation in damped composite plates," Structural Health Monitoring, 18(3), pp. 690-714.
[18] Tao, W., Shaopeng, L., Junhua, S., and Yourong, L., 2016, "Health monitoring of bolted joints using the time reversal method and piezoelectric transducers," Smart Materials and Structures, 25(2).
[19] Wang, F., 2022, "Multi-Bolt looseness detection using a new acoustic emission strategy," Structural Health Monitoring, p. 14759217221110589.
[20] Yang, J., and Chang, f.-k., 2006, "Detection of bolt loosening in C–C composite thermal protection panels: II. Experimental verification," Smart Mater. Struct, 15, pp. 591-599.
[21] Wang, T., Song, G., Wang, Z., and Li, Y., 2013, "Proof-of-concept Study of Monitoring Bolt Connection Status using a Piezoelectric based Active Sensing Method," Smart Materials and Structures, 22, p. 087001.
[22] Su, Z., Zhou, C., Hong, M., Wang, Q., and Qing, X., 2014, "Acousto-Ultrasonics-based Fatigue Damage Characterization: Linear versus Nonlinear Signal Features," Mechanical Systems and Signal Processing, 45, pp. 225–239.
[23] Lim, H. J., and Sohn, H., 2019, "Online fatigue crack prognosis using nonlinear ultrasonic modulation," Structural Health Monitoring, 18(5-6), pp. 1889-1902.
[24] Liu, P., Yang, L., Yi, K., Kundu, T., and Sohn, H., 2022, "Application of nonlinear ultrasonic analysis for in situ monitoring of metal additive manufacturing," Structural Health Monitoring, p. 14759217221113447.
[25] Zhang, M., Shen, Y., Xiao, L., and Qu, W., 2017, "Application of subharmonic resonance for the detection of bolted joint looseness," Nonlinear Dynamics, 88(3), pp. 1643-1653.
[26] Yang, Y., Ng, C.-T., and Kotousov, A., 2018, "Bolted joint integrity monitoring with second harmonic generated by guided waves," Structural Health Monitoring, 18(1), pp. 193-204.
[27] Zhang, Z., Liu, M., Liao, Y., Su, Z., and Xiao, Y., 2018, "Contact acoustic nonlinearity (CAN)-based continuous monitoring of bolt loosening: Hybrid use of high-order harmonics and spectral sidebands," Mechanical Systems and Signal Processing, 103, pp. 280-294.
[28] Amerini, F., and Meo, M., 2011, "Structural health monitoring of bolted joints using linear and nonlinear acoustic/ultrasound methods," Structural Health Monitoring, 10(6), pp. 659-672.
[29] Zhang, Z., Xu, H., Liao, Y., Su, Z., and Xiao, Y., 2017, "Vibro-acoustic modulation (VAM)-inspired structural integrity monitoring and its applications to bolted composite joints," Composite Structures, 176, pp. 505-515.
[30] Zhang, Z., Liu, M., Su, Z., and Xiao, Y., 2017, "Continuous Monitoring of Residual Torque of Loose Bolt in a Bolted Joint," Procedia Engineering, 188, pp. 278-285.
[31] Zhang, Z., Liu, M., Su, Z., and Xiao, Y., 2016, "Quantitative evaluation of residual torque of a loose bolt based on wave energy dissipation and vibro-acoustic modulation: A comparative study," Journal of Sound and Vibration, 383, pp. 156-170.
[32] Li, N., Wang, F., and Song, G., 2020, "Monitoring of bolt looseness using piezoelectric transducers: Three-dimensional numerical modeling with experimental verification," Journal of Intelligent Material Systems and Structures, 31(6), pp. 911-918.
[33] Su, Z., Zhou, C., Hong, M., Cheng, L., Wang, Q., and Qing, X., 2014, "Acousto-ultrasonics-based fatigue damage characterization: Linear versus nonlinear signal features," Mechanical Systems and Signal Processing, 45(1), pp. 225-239.
[34] Hong, M., Su, Z., Wang, Q., and Qing, X., 2013, "Modeling nonlinearities of ultrasonic waves for fatigue damage characterization: Theory, simulation, and experimental validation," Ultrasonics, 54.